

1. Introduction

The sulfur chemistry in the Community Multiscale Air Quality (CMAQ) model (version 5.0) has been updated. Here, we describe the updates to sulfur chemistry and compare model predictions obtained with CMAQv4.7.1 and CMAQv5.0.

2. Methodology

Air quality simulations were performed for January and July 2002 using CMAQv4.7.1 (Foley et al., 2010) and CMAQv5.0. The modeling domain covered the continental US using 36-km horizontal grid resolution and contained 24 vertical layers. The off-line photolysis option was used for both simulations. The non-urban as well as the urban minimum eddy diffusion coefficient has been revised in CMAQv5.0. For this study, both coefficients in CMAQv5.0 were replaced with the values in CMAQv4.7.1. Monthly mean boundary values were used for both simulations.

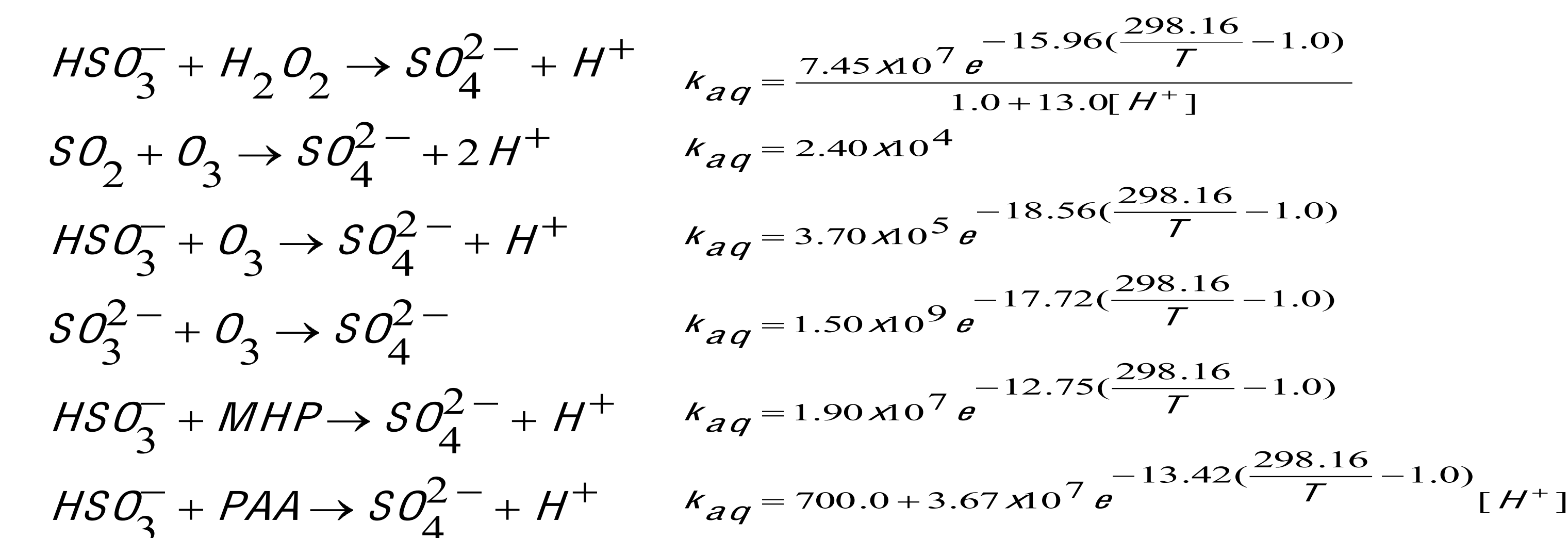
Meteorological fields were obtained from the PSU/NCAR MM5 system (Grell *et al.*, 1994) (version 3.5). Anthropogenic emissions were obtained from the National Emissions Inventory. Biogenic emissions were estimated using the Biogenic Emissions Inventory System version 3.14 (Schwede et al., 2005).

3. Sulfur chemistry in CMAQv5.0

A number of updates have been implemented in CMAQv5.0 that directly impact sulfate production potential. In CMAQv5.0, ISORROPIA 2.1 (Fountoukis and Nenes, 2007) was implemented, along with an updated treatment and tracking of crustal species (e.g., Ca²⁺, K⁺, Mg²⁺) and trace metals (e.g., Fe, Mn). These species impact aqueous-phase oxidation of S(IV) to S(VI) by altering the pH and ionic strength of the droplets, and, in the case of Fe and Mn, also affect Fe(III)/Mn(II) metal-catalyzed aqueous-phase sulfur oxidation.

The CB05 mechanism in CMAQ contains one gas-phase chemical reaction for SO₂ oxidation. The rate constant for the reaction in CMAQv5.0 has been updated using the 2006 NASA/JPL recommendation. The gas-phase rate constant for the SO₂ oxidation is now consistent between the CB05 and SAPRC07 mechanisms.

Additionally, CMAQ contains five aqueous-phase chemical pathways for SO₂ oxidation involving (1) H₂O₂, (2) O₃, (3) methylhydroperoxide (MHP), (4) peroxyacetic acid (PAA), and (5) metal catalysis. Rate constants for all pathways (except metal catalysis) have been updated following Jacobson (1997).



The rate constant for SO₂ oxidation via metal catalysis has been updated following Martin and Goodman (1991):

$$-\frac{d[S(IV)]}{dt} = 750[Mn(II)][S(IV)] + 2600[Fe(III)][S(IV)] + 1.0 \times 10^{10}[Fe(III)][Mn(II)][S(IV)]$$

In previous versions of the CMAQ model, sulfate production via the above reaction was calculated using the prescribed background concentrations of 0.01 μg/m³ for Fe(III) and 0.005 μg/m³ for Mn(II). As CMAQv5.0 contains predictions of Fe and Mn, these tracked concentrations are now used to estimate Fe(III) and Mn(II) values for the metal catalyzed oxidation pathway. To estimate aqueous-phase Fe(III) and Mn(II) concentrations from total (activated) aerosol iron and manganese, the solubility and oxidation state of these species need to be estimated. Iron solubility and oxidation state is highly variable and dependent on a number of factors including origin of the aerosol and time of day, with more soluble iron aerosol found in anthropogenic source regions compared to those areas with high levels of natural dust emissions (Alexander et al., 2009; Seifert et al., 1998). Manganese is typically more soluble than iron and exists mainly as Mn(II) in cloud/fog droplets; whereas iron cycles diurnally, and exists mainly as Fe(II) during the day and Fe(III) at night (Alexander et al., 2009). In CMAQv5.0, the solubility of iron and manganese is kept constant at 10% and 50%, respectively (Alexander et al., 2009). All dissolved manganese is assumed to be Mn(II), and Fe(III) is assumed to be 90% of the dissolved Fe at night and 10% during the day. Note that while only Fe(III) and Mn(II) impact the S(IV) oxidation rate, all Fe and Mn in the activated droplets is subjected to scavenging/deposition.

4. Results

Monthly mean surface aerosol sulfate concentrations obtained with CMAQv4.7.1 along with the predicted sulfate concentration difference between the two models are presented in Figure 1. The impact in January is mixed. CMAQv5.0 predictions increase in some locations while decrease in other locations compared to those with CMAQv4.7.1. The maximum increase in sulfate occurs just south of Lake Michigan where metal concentrations are relatively high.

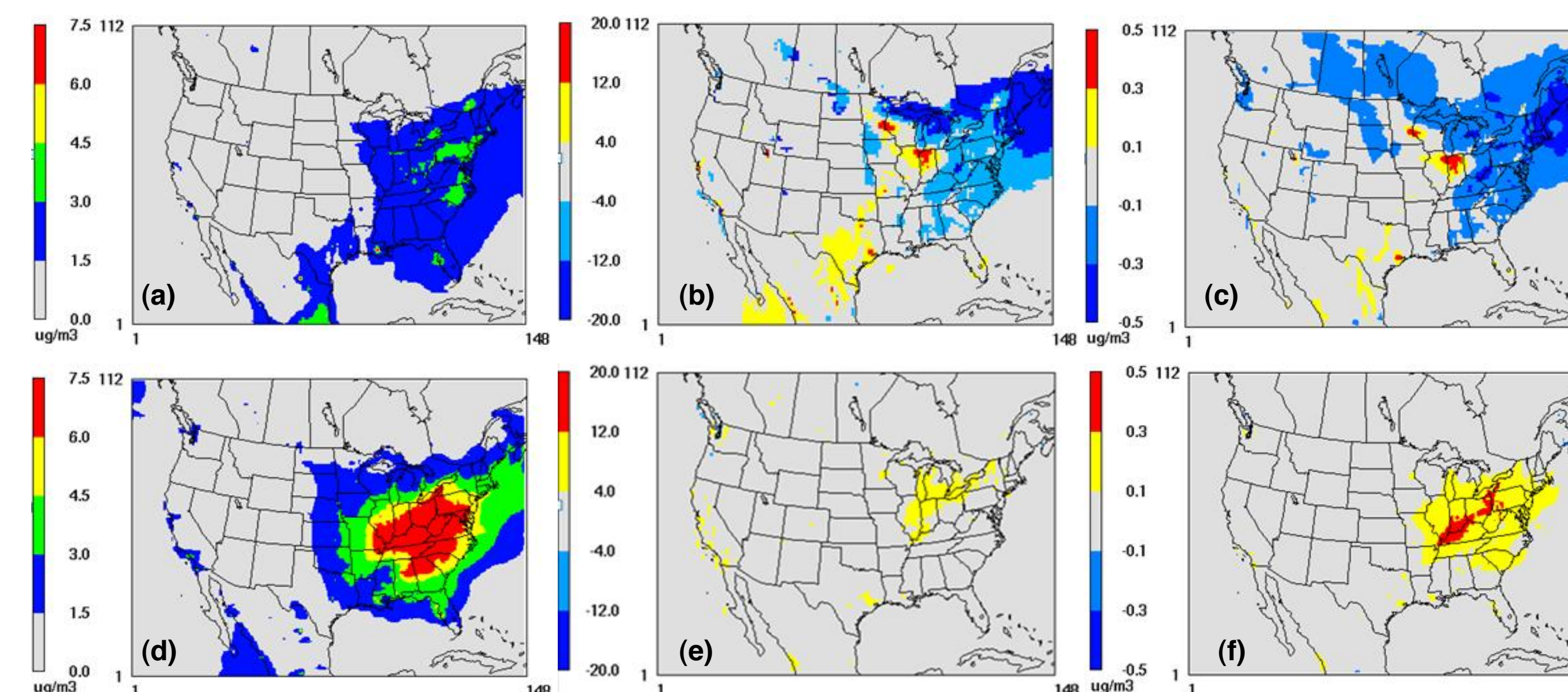


Figure 1: (a) mean aerosol sulfate with CMAQv4.7.1 in January; (b) % difference in mean aerosol sulfate between CMAQv5.0 and CMAQv4.7.1 in January; (c) absolute difference in mean aerosol sulfate between CMAQv5.0 and CMAQv4.7.1 in January; (d) mean aerosol sulfate with CMAQv4.7.1 in July; (e) % difference in mean aerosol sulfate between CMAQv5.0 and CMAQv4.7.1 in July; (f) absolute difference in mean aerosol sulfate between CMAQv5.0 and CMAQv4.7.1 in July

While monthly average concentration differences in January are $\pm 1 \mu\text{g}/\text{m}^3$, hourly differences from -12 to 34 μg/m³ were observed during the month. Percentage differences in predicted sulfate ranged between ±30%, though absolute concentration differences were not very large. In July the absolute percentage differences in sulfate predictions between the two models is smaller, but there is, on average, a more geographically widespread increase in predicted sulfate with CMAQv5.0. Monthly average CMAQv5.0 predictions increase by up to 0.5 μg/m³ in July compared to those with CMAQv4.7.1, and hourly sulfate concentration differences ranged between -5.5 and 15 μg/m³.

Monthly mean SO₂ concentrations simulated with CMAQv4.7.1 and changes between the two model predictions are presented in Figure 2. Predicted SO₂ with CMAQv5.0 generally increases in January and decreases in July compared to those with CMAQv4.7.1, correlating well with the above trends in sulfate concentrations.

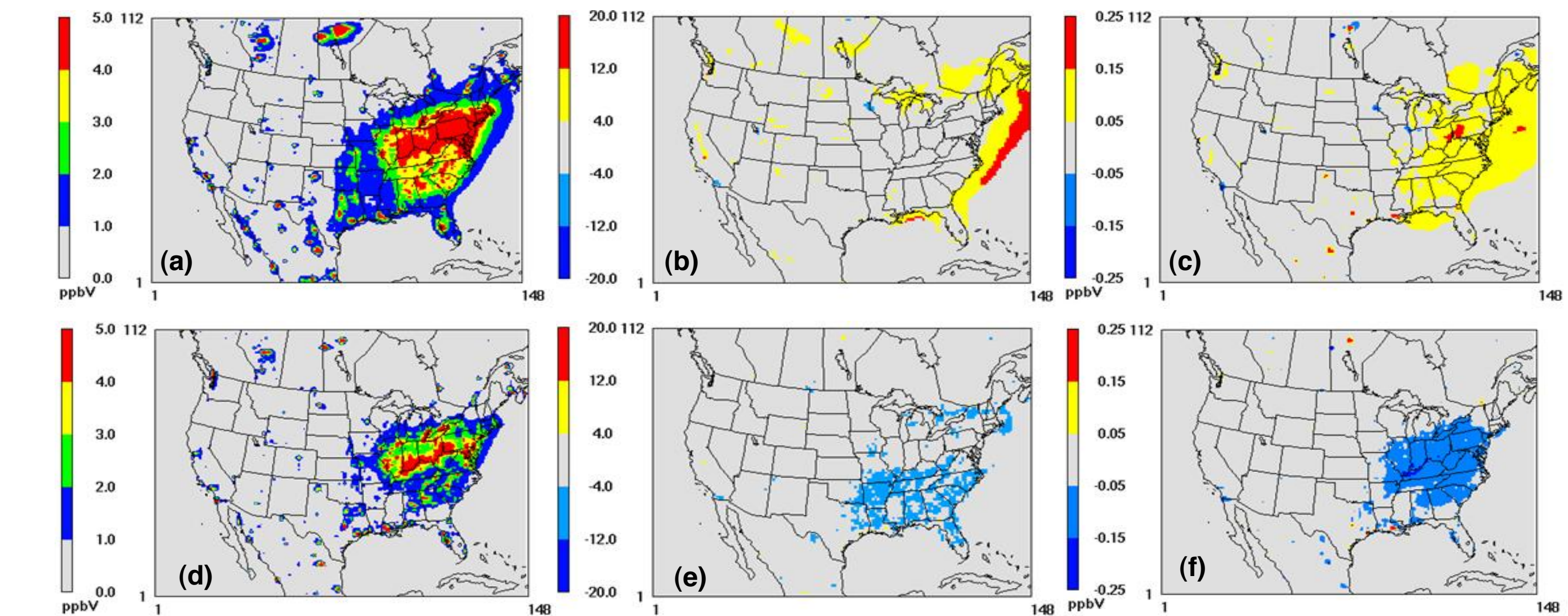


Figure 2: (a) mean SO₂ with CMAQv4.7.1 in January; (b) % difference in mean SO₂ between CMAQv5.0 and CMAQv4.7.1 in January; (c) absolute difference in mean SO₂ between CMAQv5.0 and CMAQv4.7.1 in January; (d) mean SO₂ with CMAQv4.7.1 in July; (e) % difference in mean SO₂ between CMAQv5.0 and CMAQv4.7.1 in July; (f) absolute difference in mean SO₂ between CMAQv5.0 and CMAQv4.7.1 in July

Normalized mean bias and normalized mean error for sulfate obtained with CMAQv4.7.1 and CMAQv5.0 are shown in Table 1. Normalized mean bias obtained with CMAQv5.0 improved in both January and July. Normalized mean error was similar for both models, with CMAQv5.0 having slightly lower relative error in July and higher in January compared to CMAQv4.7.1.

Table 1: Normalized mean bias and normalized mean error for CMAQv5.0 and CMAQv4.7.1

NETWORK	MONTH	Normalized Mean Bias		Normalized Mean Error	
		CMAQv5.0	CMAQv4.7.1	CMAQv5.0	CMAQv4.7.1
IMPROVE	JANUARY	6.8	14.8	42.3	42.2
CSN	JANUARY	1.4	2.1	43.6	38.1
CASTNET	JANUARY	-4.8	1.5	23.6	21.2
IMPROVE	JULY	-18.6	-20.5	37.9	38.4
CSN	JULY	-11.7	-14.3	36.0	36.2
CASTNET	JULY	-14.7	-17.2	21.7	23.1

5. Summary

CMAQv5.0 has been updated to include the latest gas-phase and aqueous-phase SO₂ oxidation rates, as well as an expanded list of explicitly tracked species, including crustal species and trace metals. On a monthly average basis, the absolute impacts on simulated sulfate concentrations are relatively small though not insignificant, and in certain regions and at shorter timescales, more significant impacts are simulated. Higher absolute differences were simulated in January, with the model updates leading to higher monthly average concentrations in some areas (e.g., near Chicago) and lower concentrations in others (e.g., the Northeastern U.S.). July showed a more widespread average increase of sulfate throughout the domain due to CMAQv5.0 updates. Model performance statistics for sulfate generally improved with CMAQv5.0. We plan to examine the impact of additional chemical reactions and meteorological conditions on sulfate in the future.

6. References

Alexander, B., R.J. Park, D.J. Jacob, S. Gong, 2009. Transition metal-catalyzed oxidation of atmospheric sulfur: global implications for the sulfur budget, *GRL*, 114, D02309.

Foley, K. M., S. J. Roselle, K.W. Appel, P. V. Bhavsar, J. E. Pleim, T. L., Otte, R. Mathur, G. Sarwar, J. O. Young, R. C. Gilliam, C. G. Nolte, J. T. Kelly, A.B. Gilliland, and J. O. Bash, 2010. Incremental testing of the Community Multiscale Air Quality (CMAQ) modeling system version 4.7, *Geosci. Model Dev.*, 3, 205–226.

Fountoukis C. and A. Nenes, 2007. ISORROPIA II: a computationally efficient thermodynamic equilibrium model for K⁺-Ca²⁺-Mg²⁺-NH₄⁺-Na⁺-SO₄²⁻-NO₃⁻-Cl⁻-H₂O aerosols. *Atmospheric Chemistry and Physics*, 7, 4639–4659.

Grell, G., J. Dudhia, and D. Stauffer, 1994. A description of the fifth-generation Penn State/NCAR Mesoscale model (MM5). NCAR Tech. Note NCAR/TN-398+STR, 122 pp.

Jacobson, M., 1997. Development and application of a new air pollution modeling system II. Aerosol module structure and design. *Atmospheric Environment*, 31, 131–144.

Martin, R.L. and T.W. Good, 1991. Catalyzed oxidation of sulfur dioxide in solution: the iron-manganese synergism, *Atmospheric Environment*, 25A, 2395–2399.

Schwede, D., G. Pouliot, and T. Pierce, 2005. Changes to the biogenic emissions inventory system version 3 (BEIS3), 4th Annual CMAS Models-3 Users' Conference, September 26–28, 2005, UNC-Chapel Hill, NC.

Seifert, R.L., A. M. Johansen, M. R. Hoffman, and S.O. Pehkonen, 1998. Measurements of trace metal (Fe, Cu, Mn, Cr) oxidation states in fog and stratus clouds, *J. Air and Waste Manage. Assoc.*, 48, 128–143.